ISSN 0036-0236, Russian Journal of Inorganic Chemistry, 2023, Vol. 68, No. 7, pp. 911–922. © Pleiades Publishing, Ltd., 2023.
ISSN 0036-0236, Russian Journal of Inorganic Chemistry, 2023. © Pleiades Publishing, Ltd., 2023.
Russian Text © The Author(s), 2023, published in Zhurnal Neorganicheskoi Khimii, 2023, Vol. 68, No. 7, pp. 975–987.

INORGANIC MATERIALS AND NANOMATERIALS

In commemoration of the 300th anniversary of St. Petersburg State University's founding

Ceramics of the Cs_2O–Al_2O_3 System Prepared by Solid-Phase Technology and the Glycine–Nitrate Combustion Process

A. V. Fedorova[a], *, V. A. Stolyarov[a], M. E. Pavelina[a], P. D. Kolonitskii[a], S. O. Kirichenko[a], A. V. Timchuk[b], and V. L. Stolyarova[a]

[a] *St. Petersburg State University, St. Petersburg, 199034 Russia*

[b] *St. Petersburg State Electrotechnical University "LETI" named after V.I. Ul'yanov (Lenin), St. Petersburg, 197022 Russia*

**e-mail: avfiodorova@gmail.com*

Received February 20, 2023; revised March 17, 2023; accepted March 20, 2023

Abstract—Cs_2O–Al_2O_3 ceramic samples containing 20 and 33 mol % cesium oxide were prepared by ceramic technique and by the glycine–nitrate combustion process. The prepared samples were identified and characterized by X-ray powder diffraction and X-ray fluorescence analyses, scanning electron microscopy, and differential thermal analysis. X-ray powder diffraction and scanning electron microscopy showed that the phase composition and surface of the samples change significantly and nonmonotonically depending on the synthetic method used and the heat treatment parameters of the batch. Optimal synthetic conditions and heat treatment parameters for preparing Cs_2O–Al_2O_3 samples were elucidated.

DOI: 10.1134/S0036023623600909

INTRODUCTION

Despite the large amount of literature on oxo- and hydroxo aluminum compounds, works aimed at developing methods for preparing, studying, and using oxide alumina-base ceramics are still relevant [1–3]. This relevance is due to the high chemical, thermal, and mechanical stability of alumina [4–6] and its rich polymorphism [7–9].

The Cs_2O–Al_2O_3 system is the least studied of the alumina-comprising systems. In recent years, however, approaches have been successfully implemented to the preparation of europium-doped luminescent ceramics $CsAlO_2 : Eu^{3+}$ [10], nanosized $CsAlO_2$ particles, which are candidates for use in optical devices [11], and Cs_2O–Al_2O_3 catalysts [12, 13]. A feature of cesium oxide systems is the ability to form X-ray amorphous and glassy states [14, 15], with attendant difficulties in choosing the synthetic approach to the manufacture of cesium oxide–containing ceramics. Despite the high scientists' and practitioners' interest in aluminum oxide and cesium oxide ceramics, the phase diagram for the Cs_2O–Al_2O_3 system is not yet available [16].

Characteristic features of the Cs_2O–Al_2O_3 system are the hygroscopicity of oxo cesium compounds, the dependence of the alumina crystal structure on the synthetic methods and parameters, and the volatility of cesium compounds at high temperatures [17, 18].

The factors were responsible for the recognition of the problem to choose the optimal and adequate method for preparing Cs_2O–Al_2O_3 samples. Ceramic technique is a priority method for the synthesis of oxide ceramics [19–22]. The benefits of this method are known to include its rapidity and ease of embodiment. The method consists in homogenization of the mixture of precursor materials and subsequent calcination of the homogenized mixture at high temperatures. Since diffusion is a low-rate process in solid-phase technology, it is extremely important to achieve a uniform distribution of the reagents throughout the volume of the batch during homogenization. In some cases, this is not an optimal approach, and then one has to use what we call chemical homogenization in aqueous solutions [23, 24].

Along with ceramic technique, another widely used process is glycine–nitrate combustion [24, 25], where product particles are formed in the course of short-term combustion of the batch [24, 25]. The underlying idea of the method is a redox reaction in aqueous solution between nitrate ions and glycine. Since glycine plays both the role of an oxidizing agent and the role of an organic fuel, special attention is paid to its amount

necessary for synthesis, which is individual depending on the chemical nature of the system [26].

In view of the unavailability of a phase diagram for the Cs_2O–Al_2O_3 system and the hygroscopicity and volatility of cesium, our goal in this work was to study the usefulness of ceramic technique and the glycine–nitrate combustion process for manufacturing Cs_2O–Al_2O_3 ceramic samples containing 20 and 33 mol % cesium oxide with subsequent identification of the thus-prepared samples.

EXPERIMENTAL

The chemicals used to prepare test ceramic samples by ceramic technique technology were γ-Al_2O_3 prepared in a laboratory and Cs_2CO_3 (99.9%, chemically pure grade, TU 6-09-638-80, Russia). The γ-Al_2O_3 low-temperature phase was prepared via thermolysis of $Al(NO_3)_3 \cdot 9H_2O$ (97%, pure grade, GOST (State Standard) 3757-75, Russia) at 573 K. The cesium carbonate was calcined at 1073 K for 12 h prior to use.

According to the ceramic technique, calculated amounts of cesium carbonate and γ-Al_2O_3 were homogenized together with an agate mortar and a pestle for 1 h. Due to the hygroscopicity of cesium carbonate, the precursors were triturated with isopropanol. Since the parameters of solid-phase reactions to prepare Cs_2O–Al_2O_3 samples are not available in the literature, the amount of isopropanol for the homogenization of the reagents was selected experimentally. In order to identify the effect of the amount of isopropanol on the characteristics (phase composition and surface morphology) of samples that were prepared by ceramic technique, a smaller amount of isopropanol was used to homogenize the calculated amounts of reagents for a 20 mol % cesium oxide sample than for a 33 mol % cesium oxide sample. The amount of isopropanol taken to prepare the 33 mol % cesium oxide sample was greater than calculated for the batch.

The thus-prepared batch was pressed into tablets using a organic glass mold, and the tablets calcined in a muffle furnace in open corundum crucibles at the temperatures and for the times as follows: at 773 K, for 15 h; at 873 K, for 10 h; at 973 K, for 15 h; at 1073 K, for 10 h; and at 1373 K, for 10 h. Once fulfilled, each of those annealing steps was followed by X-ray powder diffraction and X-ray fluorescence analyses to study phase and elemental compositions.

In view of the exceptionally high tendency of cesium oxide to evaporate, glycine–nitrate combustion was also chosen as an alternative method for preparing test samples. The precursors used to prepare Cs_2O–Al_2O_3 samples containing 20 mol % cesium oxide via glycine–nitrate combustion were Cs_2CO_3 (99.9%, chemically pure grade, TU 6-09-638-80, Russia) and $Al(NO_3)_3 \cdot 9H_2O$ (97%, pure grade, GOST (State Standard) 3757-75, Russia). The calculated amounts of the precursors were dissolved in dilute nitric acid under constant heating on a sand bath. The water-to-acid ratio was 1 : 2 vol/vol. After the precursors dissolved completely, glycine was added to the solution in the ratio (n_i): $n_{Cs_2CO_3} : n_{Al(NO_3)_3 \cdot 9H_2O} : n_{C_2H_5NO_2}$ = 1.0 : 8.1 : 17.2 mol/mol; afterwards, heating continued to remove the solvent until the mixture boiled. After the solvent evaporated upon boiling, the spontaneous combustion of the reaction mixture was observed. Once the combustion was over, the mixture was a white fine powder with dark inclusions of carbon; the powder was compressed into tablets using an organic glass mold and then calcined in a muffle furnace at the specified temperatures for the specified times: at 773 K, for 15 h; at 873 K, for 10 h; at 973 K, for 15 h; at 973 K, for 365 h; and at 973 K, for 870 h. Each calcination was followed by the X-ray powder diffraction and X-ray fluorescence analyses of the test samples in order to determine their phase and quantitative compositions.

The glycine–nitrate combustion process was also used to prepare 33 mol % cesium oxide samples of the Cs_2O–Al_2O_3 system. The precursors used were $CsNO_3$ (CAS Sample no. 7789-18-6, 99.9%, chemically pure grade, TU 6-09-437-75, Russia) and $Al(NO_3)_3 \cdot 9H_2O$ (97%, pure grade, GOST (State Standard) 3757-75, Russia). After the calculated amounts of metal nitrates dissolved in distilled water, glycine was added to the solution in the molar ratio calculated as

$$n(C_2H_5NO_2) = 5\sum n(NO_3^-)/9,$$

where n is the number of moles of the reducing agent per mole of the product [27].

It should be mentioned here that the amounts of metal nitrates and glycine to be taken to prepare the 33 mol % cesium oxide sample were calculated to ensure a lower intensity of batch combustion. The thus-produced mixtures were compressed into tablets and then calcined at the specified temperatures for the specified times: at 773 K, for 15 h; at 873 K, for 10 h; at 973 K, for 15 h; at 1073 K, for 10 h; at 973 K, for 365 h; and at 973 K, for 870 h. As in the preceding case, the samples were identified by X-ray powder diffraction and X-ray fluorescence analyses after each calcination step.

The samples prepared under the conditions specified in Table 1 were identified and characterized by X-ray powder diffraction and X-ray fluorescence analyses, scanning electron microscopy, and differential thermal analysis to be used further to study the physicochemical properties of the Cs_2O–Al_2O_3 system.

X-ray powder diffraction experiments were carried out on a Bruker D2 Phaser diffractometer with a copper cathode (Cu$K_{\alpha 1,2}$ radiation, voltage: 30 kV) and a Rigaku Ultima IV diffractometer with a cobalt cathode.

X-ray fluorescence analysis was performed on an EDX 800 HS (Shimadzu) energy-dispersive X-ray

Table 1. Synthetic parameters for preparing Cs_2O–Al_2O_3 ceramic samples

Sample no.	As-synthesized ratio Cs_2O : Al_2O_3, mol %	Synthetic method	Precursors	T, K	Synthesis time τ, h
1	20 : 80	Ceramic technique	Cs_2CO_3 γ-Al_2O_3	773	15
2				873	10
3				973	15
4				973	365
5				973	870
6				1073	10
7				1373	10
8	33 : 67	Ceramic technique with an excess of isopropanol	Cs_2CO_3 γ-Al_2O_3	773	15
9				873	10
10				973	15
11				973	365
11a				383	2
12				973	870
13				1073	10
14				1373	10
15	20 : 80	Glycine–nitrate combustion	Cs_2CO_3 $Al(NO_3)\cdot 9H_2O$	773	15
16				873	10
17				973	15
18				973	365
19				973	870
20				1073	10
21	33 : 67	Glycine–nitrate combustion	$CsNO_3$ $Al(NO_3)\cdot 9H_2O$	773	15
22				873	10
23				973	15
24				973	365
25				973	870
26				1073	10

fluorescence spectrometer in vacuo in the range of characteristic lines of the elements from carbon through uranium.

The surfaces of samples were studied using a Hitachi S-3400N scanning electron microscope equipped with an Oxford Instruments X-Max 20 spectrometer for energy-dispersive analysis.

High-resolution electron microscopic observations were performed using a Zeiss Merlin scanning electron microscope with a field-mission cathode, a Gemini-II electron optics column, and an oil-free vacuum system. ln-lens SE and SE2 secondary electron detectors were used to record signals. An Oxford Instruments INCAx-act X-ray microanalysis attachment was used for microanalysis.

The high-temperature thermal analysis of Cs_2O–Al_2O_3 samples was performed on a Shimadzu DTG-60 thermal analyzer in the range 298–1373 K. Samples for thermoanalytical experiments were thin disks compressed under 200 atm, whose fragments were placed in a platinum crucible. A blank run with empty crucibles preceded the thermoanalytical experiments in order to correct the signals from test samples after records.

RESULTS AND DISCUSSION

X-ray Powder Diffraction Analysis

Ceramic technique and glycine–nitrate combustion process with various precursors and various heat-treatment conditions, namely, temperature T and time τ, were used to prepare Cs_2O–Al_2O_3 samples containing 20 and 33 mol % cesium oxide. The compositions and numbering of the test samples, together with the synthetic methods and parameters for each sample,

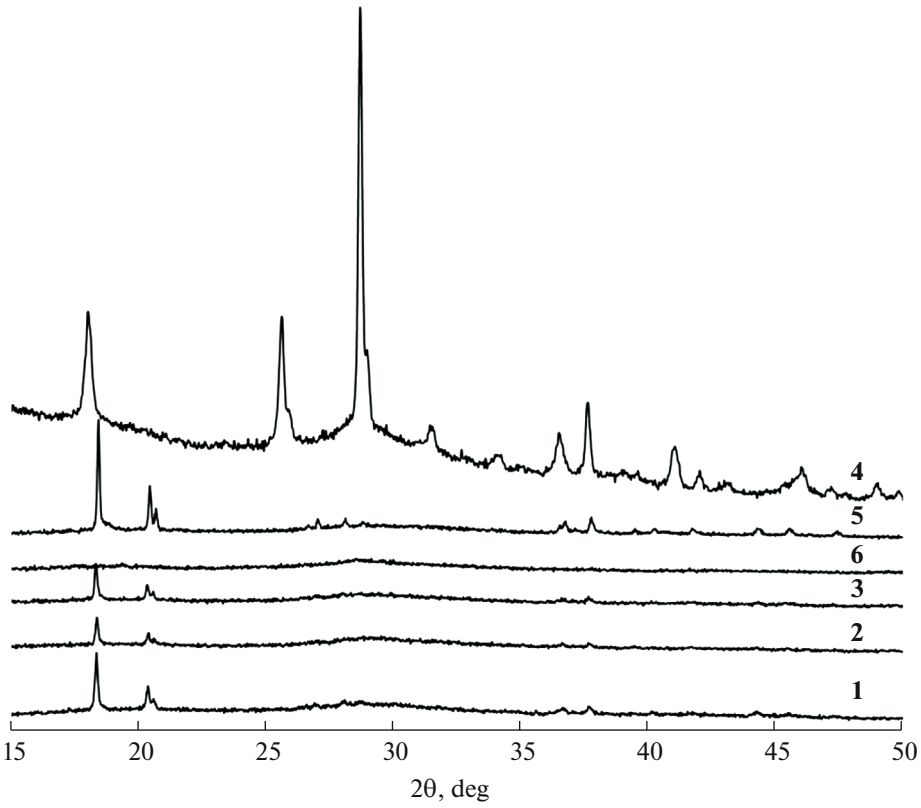

Fig. 1. X-ray diffraction patterns of Cs_2O–Al_2O_3 samples containing 20 mol % cesium oxide that were prepared by ceramic technique from Cs_2CO_3 and γ-Al_2O_3 with various batch calcination parameters (Table 1).

are found in Table 1. The numbering of samples as in Table 1 will be used further in the text.

Figures 1–4 show the X-ray diffraction patterns of the prepared Cs_2O–Al_2O_3 samples. The X-ray diffraction patterns in Fig. 1 refer to samples **1**–**6**, which are Cs_2O–Al_2O_3 samples containing 20 mol % cesium oxide that were prepared by ceramic technique from Cs_2CO_3 and γ-Al_2O_3 with isopropanol trituration. The batch was calcined at various (temperature and time) conditions. X-ray powder diffraction showed that all as-synthesized samples were more than 80% amorphous. Therefore, further phase identification in the prepared samples was difficult.

The sample calcined at 973 K for 365 h (sample **4**) contained the greatest amount of a crystallized phase in comparison to the samples prepared by the same method but under other isothermal exposure conditions. The diffraction peaks in sample **4** appeared at 2θ = 28.75°, 25.64°, 37.67°, 18.33°, and 20.35°; they can be identified with the strongest peaks of aluminum hydroxide crystal phases: $Al(OH)_3$ (gibbsite) (14, $P121/n1$, ICDD PDF-2 Release 2011, Sample no. 01-080-7022), triclinic $Al(OH)_3$ (2, $P\bar{1}$, ICDD PDF-2 Release 2016, RDB Sample no. 01-077-9948), or eta-Al_2O_3 (227, $Fd\bar{3}m$, ICDD PDF-2 Release 2016, RDB, Sample no. 00-056-0458), or with $CsAlO_2$ (227, $Fd\bar{3}m$, ICDD PDF-2 Release 2016, RDB, Sample no. 01-074-2291). An elevation of the batch calcination temperature to 1073 K yields an X-ray amorphous sample (sample **6**).

It should be noted that, in all samples containing a large amount of the X-ray amorphous phase, low-intensity diffraction peaks were identified at the crystal-rotation angles 2θ corresponding to the major diffraction peaks of the crystalline phases found earlier in sample **4**.

In the X-ray diffraction pattern of the 20 mol % cesium oxide sample of the Cs_2O–Al_2O_3 system prepared by standard ceramic technique and then calcined at 1373 K for 10 h (sample **7**), the only crystalline phase was α-Al_2O_3. This means that the chosen batch calcination temperature did not provide the preparation of Cs_2O–Al_2O_3 samples.

Therefore, batch calcination at 973 K with 365-h isothermal exposure is the optimal schedule for providing the highest crystallinity of Cs_2O–Al_2O_3 ceramic samples prepared by ceramic technique from Cs_2CO_3 and γ-Al_2O_3 comprising trituration with isopropanol.

Figure 2 shows the X-ray diffraction patterns for 33 mol % Cs_2O samples of the Cs_2O–Al_2O_3 system that were prepared by solid-phase technology from

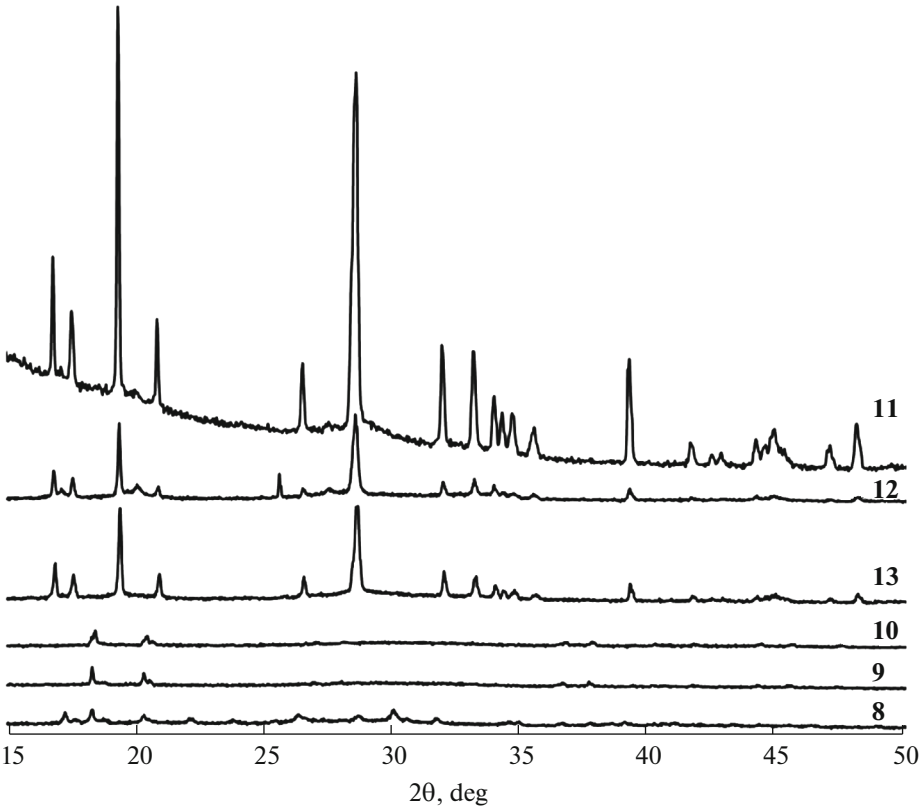

Fig. 2. X-ray diffraction patterns of Cs_2O–Al_2O_3 samples containing 33 mol % Cs_2O that were prepared by ceramic technique from Cs_2CO_3 and γ-Al_2O_3 with various batch calcination parameters (Table 1).

Cs_2CO_3 and γ-Al_2O_3 with trituration with excess isopropanol. In the samples that were prepared with batch calcination at 773 K for 15 h (sample **8**), at 873 K for 10 h (sample **9**), and at 973 K for 15 h (sample **10**), X-ray powder diffraction patterns showed the predominance of an X-ray amorphous phase with low-intensity diffraction peaks. The reflection peak positions for these samples correspond to the $Al(OH)_3$ (gibbsite) structure (14, *P*121/*n*1, ICDD PDF-2 Release 2011, Sample no. 01-080-7022). It should be emphasized that powder samples **8**–**10** blurred while interacting with moisture upon prolonged contact with air, and passed into a plasticine-like state.

The X-ray diffraction patterns for samples that were prepared with a long-term isothermal exposure of 365 h (sample **11**) or 870 h (sample **12**) at 973 K or of 10 h (sample **13**) at 1073 K, are typical of multiphase samples. The major diffraction peaks for those samples appeared at 2θ = 28.345°, 18.645°, 33.156°, 34.125°, 14.458°, and 12.489°. These diffraction peaks lie in the range where the diffraction peaks appear from $Al(OH)_3$ (gibbsite) (14, *P*121/*n*1, ICDD PDF-2 Release 2011, Sample no. 01-080-7022), γ-Al_2O_3 [28], and cubic cesium aluminate $CsAlO_2$ (227, $Fd\bar{3}m$, ICDD PDF-2 Release 2016, Sample no. 01-074-2291) [29].

Figure 3 shows the X-ray diffraction patterns for samples **15**–**20**, which are 20 mol % Cs_2O samples of the Cs_2O–Al_2O_3 system that were prepared by the glycine–nitrate combustion process from Cs_2CO_3 and $Al(NO_3)_3 \cdot 9H_2O$ with various calcination (temperature and time) conditions. Noteworthy, the X-ray diffraction patterns of this set of samples (sample **15**) feature a relatively small amount of an X-ray amorphous phase even at 773 K, unlike in the samples of the same composition prepared by solid-phase technology. Moreover, long-term (365-h) calcination at 973 K made the crystalline phase to disappear (in sample **18**). The only way to achieve the formation of a crystalline phase in samples prepared by this method is via batch calcination at 973 K for 870 h (sample **19**). The major diffraction peaks for this sample appeared at 2θ = 28.701°, 18.008°, 25.535°, and 37.632°; they correspond to the aluminum hydroxide $Al(OH)_3$ (gibbsite) crystallized phase (14, *P*121/*n*1, ICDD PDF-2/Release 2011, Sample no. 01-080-7022). High-resolution X-ray diffraction showed low-intensity peaks of triclinic $Al(OH)_3$, α-Al_2O_3, and $Cs_2(Al_2O(OH)_6$ in this sample.

Figure 4 shows the X-ray diffraction patterns for samples **21**–**26**, which are 33 mol % Cs_2O samples of the Cs_2O–Al_2O_3 system that were prepared by the gly-

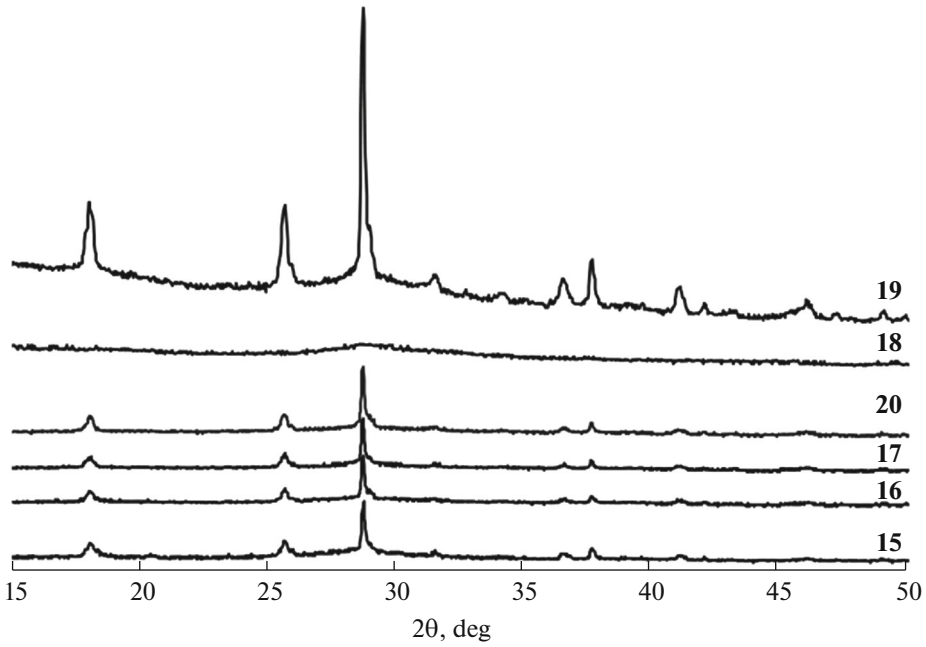

Fig. 3. X-ray diffraction patterns of Cs_2O–Al_2O_3 samples containing 20 mol % Cs_2O that were prepared by the glycine–nitrate combustion process from Cs_2CO_3 and $Al(NO_3)_3 \cdot 9H_2O$ with various batch calcination parameters (Table 1).

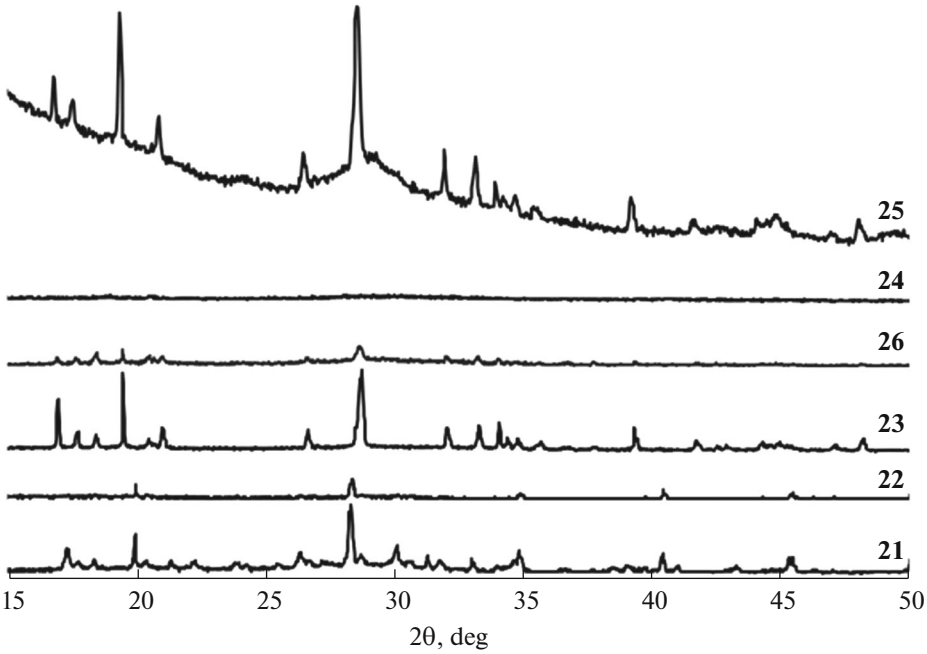

Fig. 4. X-ray diffraction patterns of Cs_2O–Al_2O_3 samples containing 33 mol % Cs_2O that were prepared by the glycine–nitrate combustion process from $CsNO_3$ and $Al(NO_3)_3 \cdot 9H_2O$ with various batch calcination parameters (Table 1).

cine–nitrate combustion process from $CsNO_3$ and $Al(NO_3)_3 \cdot 9H_2O$ with various batch calcination (temperature and time) conditions. Sample **21**, which was calcined at 773 K for 15 h, contains $Al(OH)_3$ (gibbsite) and $CsNO_3$ (144, *P*31, ICDD PDF-2 Release 2020, RDB, Sample no. 01-079-0009) phases in addition to the major X-ray amorphous phase. The presence of cesium nitrate in the sample indicates that the calcination conditions were insufficient for the complete decomposition of the intermediates formed during the synthesis. Minor cesium nitrate remains in sample **22** after calcination at 873 K for 10 h, while the amount of

Table 2. Overall weight change (Δm) in Cs_2O–Al_2O_3 samples as shown by thermogravimetric analysis

Sample no.	**17**	**18**	**19**	**10**	**11**	**11a**	**24**
As-synthesized ratio Cs_2O : Al_2O_3, mol %	20 : 80	20 : 80	20 : 80	33 : 67	33 : 67	33 : 67	33 : 67
Δm	0	−24.57	−17.48	0	−36.32	−21.62	−26.82

the crystalline phase becomes smaller. Both samples take up water upon long-term contact with air to convert to plasticine-like mass. When the batch is calcined at 1073 K for 10 h, the sample enters an X-ray amorphous state (sample **26**). The X-ray diffraction pattern of sample **23**, which experienced calcination at 973 K for 15 h, corresponds to the profile of a multiphase sample and also features both an X-ray amorphous phase and a crystallized phase. The major diffraction peaks were found at 2θ = 19.495°, 28.696°, 28.786°, 16.973°, 34.128°, 39.376°, 32.112°, 21.015°, 33.366°, 26.671°, 58.539°, and 17.713°. The diffraction peaks for those samples lie in the range where the diffraction peaks of $Al(OH)_3$ (gibbsite) and cubic cesium aluminate $CsAlO_2$ appear. In sample **25**, which was calcined at 973 K for 870 h, the major diffraction peaks were found at 2θ = 28.455°, 18.645°, 33.156°, 34.125°, 14.458°, and 12.489°; they refer to $Al(OH)_3$ (gibbsite), γ-Al_2O_3, and $CsAlO_2$ crystallized phases.

The X-ray diffraction patterns of samples that were prepared with batch calcination at 1373 K for 10 h feature only an aluminum oxide phase. X-ray fluorescence analysis of the same sample verified the absence of cesium therein. Therefore, the calcination schedule at 1373 K for 10 h cannot serve to prepare Cs_2O–Al_2O_3 samples.

Thus, X-ray powder diffraction showed an X-ray amorphous phase in all Cs_2O–Al_2O_3 ceramic samples containing 20 or 33 mol % Cs_2O. The X-ray diffraction patterns of these samples are typical of multiphase systems. The amount of the crystalline phase in the sample depends on the synthetic method and heat treatment conditions.

The alumina percentage in the Cs_2O–Al_2O_3 samples containing 20 or 33 mol % Cs_2O exceeds the cesium oxide percentage. Some of the alumina can form various hydroxo species when the sample is brought in contact with water because of the hygroscopicity of cesium compounds. Two stoichiometries are typical of aluminum hydroxide: $Al(OH)_3 = Al_2O_3 \cdot 3H_2O$ and $AlO(OH) = Al_2O_3 \cdot H_2O$ [22]. These hydroxo species can each exist in two crystal phases: α and γ. Thermal dehydration of aluminum hydroxide and other aluminum hydroxo compounds can stabilize various alumina polymorphs, depending on calcination temperature, namely: α-Al_2O_3, γ-Al_2O_3, χ-Al_2O_3, θ-Al_2O_3, η-Al_2O_3, or δ-Al_2O_3. The other alumina polymorphs are low-temperature phases and are stabilized under soft synthesis settings. Amorphous $Al_2O_3 \cdot nH_2O$ of variable composition is also known. These circumstances, taken together, are responsible for the multiphase constitution and X-ray amorphous state of the prepared samples.

Differential Thermal Analysis

The differential thermal analysis was used to characterize the Cs_2O–Al_2O_3 samples containing 20 and 33 mol %cesium oxide that were prepared by ceramic technique or the glycine–nitrate combustion process in the range 298–1373 K.

Figure 5 compares DTA signal versus temperature curves for Cs_2O–Al_2O_3 ceramic samples prepared under various conditions; the curves are numbered to match sample numbering in Table 1. Sample **11a** was prepared via an additional 2-h heat treatment of sample **11** at 383 K before thermal analysis.

Thermal analysis did not detect significant weight loss in samples **10** and **17** and no thermal events in the range of temperatures from 298 to 1373 K. The DTA curves of other samples feature endotherms in the range of temperatures up to 573 K. The total weight loss for the studied samples appears in Table 2. Sample **17** is a dry ceramic powder containing 20 mol % cesium oxide; it was prepared by the glycine–nitrate combustion process with subsequent calcination at 973 K for 15 h. The powder of sample **10**, which is also moisture resistant, contains 33 mol % cesium oxide; it was prepared by solid-phase technology with isothermal exposure under the same conditions as for sample **17** (973 K for15 h).

The other studied samples featured weight loss, which could be explained by the presence of adsorbate water on their surfaces. Sample **11**, which is a Cs_2O–Al_2O_3 sample containing 33 mol % cesium oxide that was prepared by solid-phase technology with isothermal exposure at 973 K for 365 h, became moist upon a long-term contact with water. Sample **11** was predried at 383 K for 2 h before a thermoanalytical experiment (sample **11a**). The DTA curve of sample **11a** features two endotherms at 468.05 and 547.85 K; the total weight loss is 21.62%.

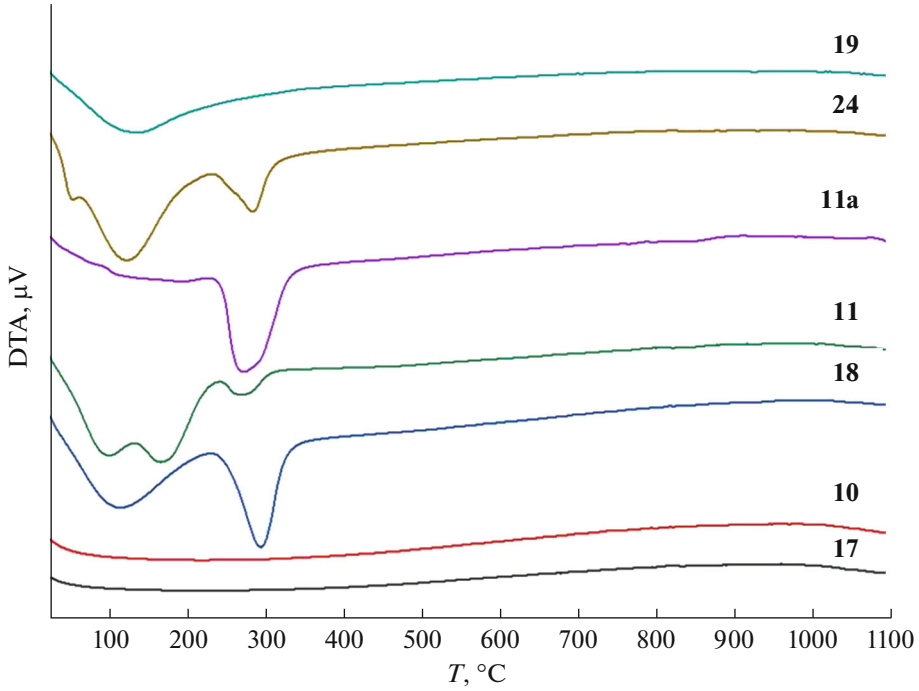

Fig. 5. Comparison of DTA signal versus temperature curves (DTA, μV) for $Cs_2O–Al_2O_3$ samples **10**, **11**, **11a**, **17–19**, and **24**.

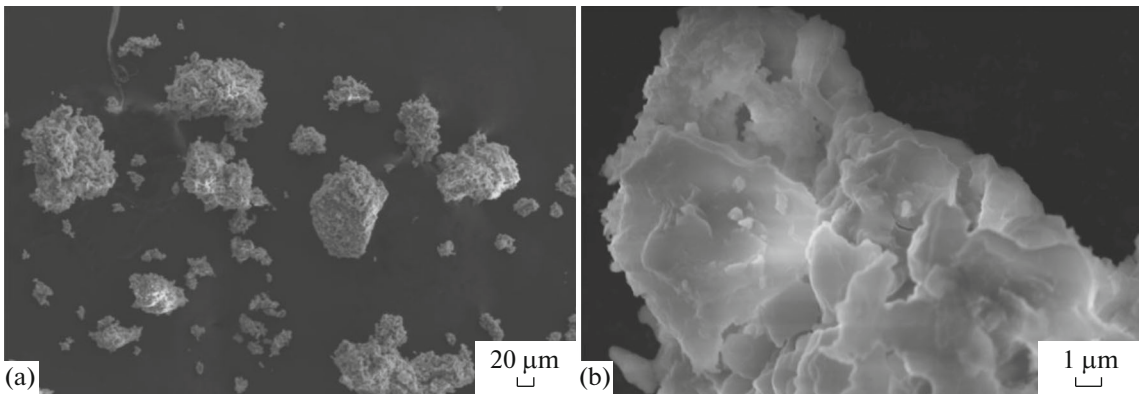

Fig. 6. Micrographs with (a) 20- and (b) 1-μm magnification taken from the surface of a $Ce_2O–Al_2O_3$ sample containing 33 mol % Cs_2O that was prepared by solid-phase technology with 15-h batch calcination at 973 K.

Surface Microscopy and X-ray Fluorescence Analysis

Figures 6–8 show the high-resolution scanning electron micrographs of $Cs_2O–Al_2O_3$ samples.

Figures 6a and 6b show surface micrographs of sample **10**, which is a 33 mol % cesium oxide sample prepared by solid-phase technology with calcination at 973 K for 15 h. The surface of the sample is represented by irregularly shaped crystal grains of various sizes. Large particles with sizes ranging within 45–150 μm amount to 28% of the total number of particles on the observed surface area of the sample. Fine particles have sizes in the range 6–45 μm and are 72% of all particles. Small-sized crystal grains, with unclear edges and coalesced, can be seen on the surface micrographs of the same sample at a magnification of up to 1 μm (Fig. 6b).

Figures 7a and 7b show the surface micrographs of sample **17**, which is a $Cs_2O–Al_2O_3$ sample containing 20 mol % Cs_2O that was prepared by the glycine–nitrate process with calcination at 973 K for 15 h. The images show entities of various shapes and of smaller sizes than those in sample **10**, which was prepared by ceramic technique. Of the particles on the observed surface area of sample **10**, 10% were particles of sizes of 20–50 μm, ca. 32% were 10–20 μm in size, and 58% were particles with sizes of at most 10 μm. The glycine–

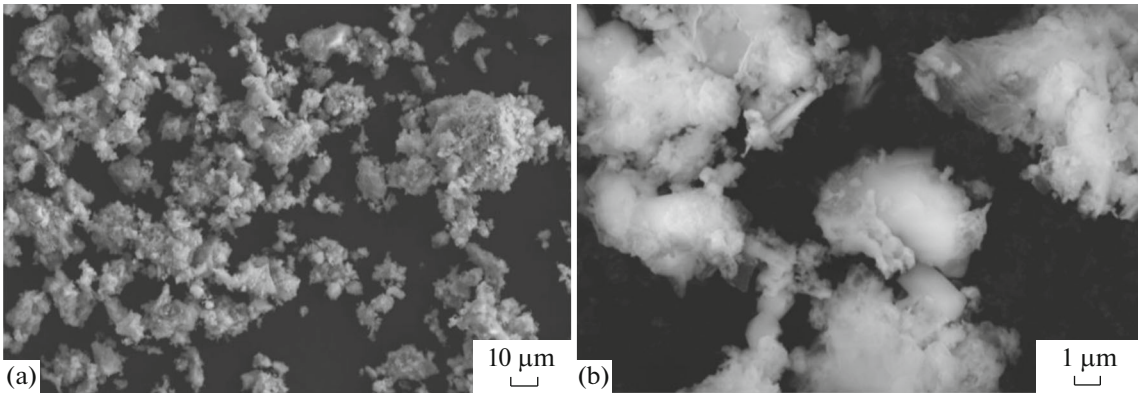

Fig. 7. Micrographs with (a) 10- and (b) 1-μm magnification taken from the surface of a Cs_2O–Al_2O_3 sample containing 20 mol % Cs_2O that was prepared by the glycine–nitrate combustion process with 15-h batch calcination at 973 K.

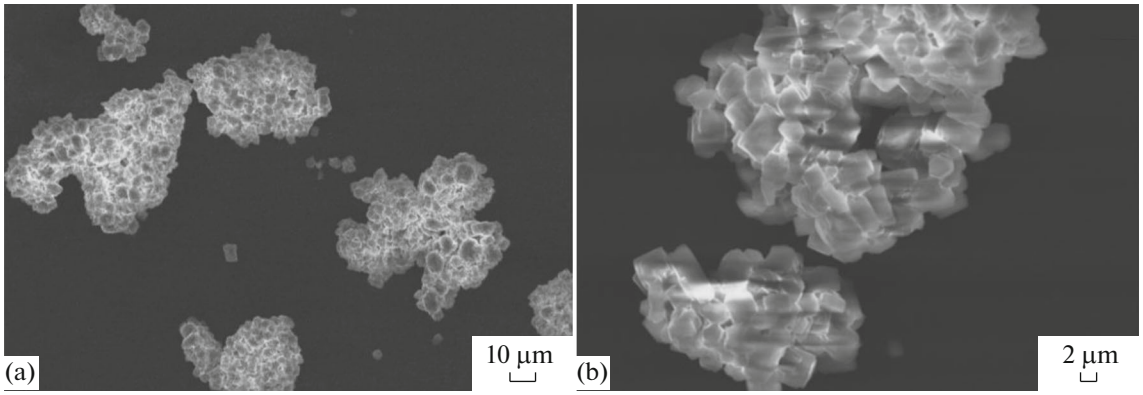

Fig. 8. Micrographs with (a) 10- and (b) 2-μm magnification taken from the surface of a Cs_2O–Al_2O_3 sample containing 33 mol % Cs_2O that was prepared by the glycine–nitrate combustion process with 15-h calcination at 973 K.

nitrate combustion process when used to prepare Cs_2O–Al_2O_3 samples yields smaller particles than those produced by ceramic technique. The micrographs of sample **17** taken under 1-μm magnification show fine grains that do not have a pronounced habit.

The surface micrographs (Figs. 8a and 8b) of sample **23**, which is a Cs_2O–Al_2O_3 sample containing 33 mol % Cs_2O that was prepared via glycine–nitrate combustion and crystallized at 973 K with 15-h isothermal exposure, show cubic grains with a well-defined habit forming agglomerates of 40–60 μm. On the micrographs of this sample taken at up to 1-μm magnification, one can distinguish cube-shaped crystal grains with 1.5–2.0 μm faces, larger grains shaped in parallelepipeds with faces a = 0.5–1.5 μm, b = 2–2.8 μm, and irregular-shaped grains having sizes less than 2.5 μm.

The elemental composition for all of the prepared samples of the studied system listed in Table 1 was determined by X-ray fluorescence spectroscopy. Figure 9 shows an energy-dispersive spectrum for one sample. Only cesium and aluminum characteristic lines were detected in all samples. The rhodium characteristic lines observed in the spectrum refer to the anode material of the instrument on which analysis was carried out.

Table 3 lists the elemental compositions of Cs_2O–Al_2O_3 ceramic samples that were prepared by ceramic technique or glycine–nitrate combustion process with subsequent heat treatment of the batch under various (temperature and time) conditions.

When the batch prepared by solid-phase technology was calcined at 1373 K for 10 h (for samples **7** and **14**), cesium completely vaporized from the batch; accordingly, the spectra of these samples featured only aluminum characteristic lines. The X-ray diffraction patterns of these samples also featured only one crystallized phase, which was identified as α-Al_2O_3. Thus, 1373 K is a too high synthesis temperature to prepare Cs_2O–Al_2O_3 oxide ceramics.

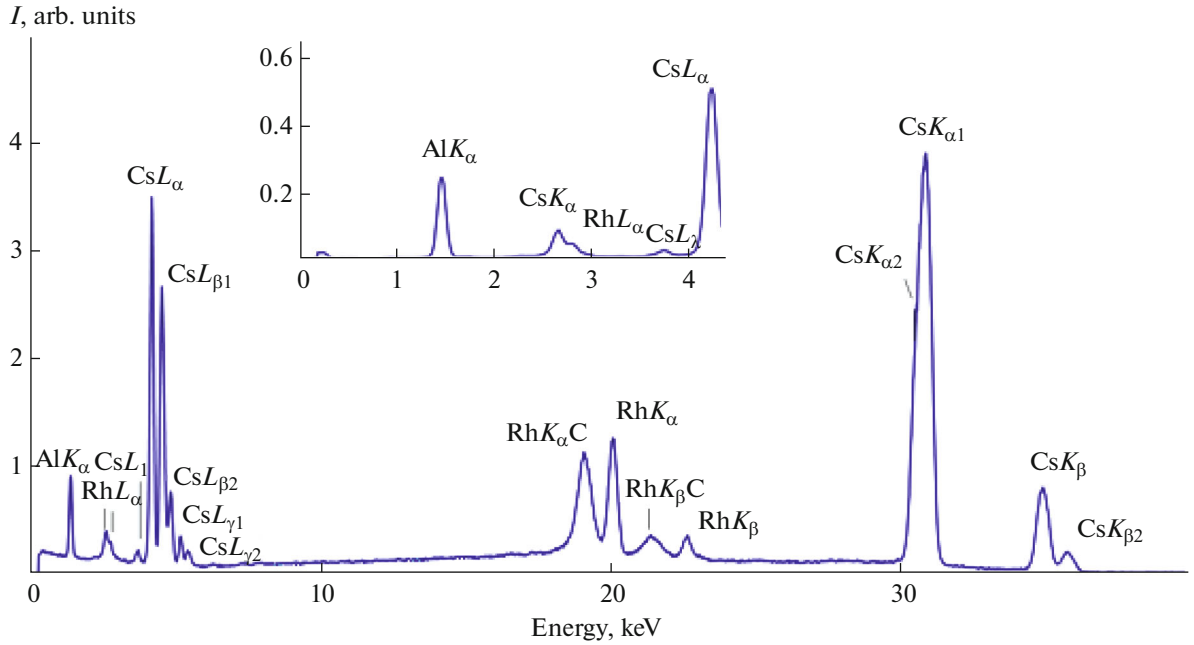

Fig. 9. Energy-dispersive spectrum of a 20 mol % Cs_2O + 80 mol % Al_2O_3 sample prepared by the glycine–nitrate combustion process.

Table 3. X-ray fluorescence analysis of Cs_2O–Al_2O_3 samples

Synthetic method			Calcination parameters		As-analyzed ratio Cs_2O : Al_2O_3, mol %	
			T, K	τ, h	Cs_2O	Al_2O_3
As-synthesized ratio Cs_2O : Al_2O_3, mol %	20 : 80	Solid-phase technology	873	10	20.18 ± 0.33	79.82 ± 1.20
			973	15	20.13 ± 0.30	79.87 ± 1.20
			973	365	19.93 ± 0.30	80.07 ± 1.20
			973	870	19.92 ± 0.30	80.08 ± 1.20
			1073	10	19.97 ± 0.30	80.03 ± 1.20
			1373	10	0	100
		Glycine–nitrate process	873	10	20.42 ± 0.31	79.58 ± 1.20
			973	15	20.14 ± 0.30	79.86 ± 1.20
			973	365	19.62 ± 0.29	80.38 ± 1.20
			973	870	19.84 ± 0.30	80.16 ± 1.20
			1073	10	19.91 ± 0.30	80.09 ± 1.20
	33 : 67	Solid-phase technology	873	10	33.80 ± 0.51	66.20 ± 0.993
			973	15	33.75 ± 0.51	66.25 ± 0.99
			973	365	33.28 ± 0.50	66.72 ± 1.00
			973	870	30.02 ± 0.45	69.98 ± 1.05
			1073	10	31.84 ± 0.48	68.16 ± 1.02
			1373	10	0	100
		Glycine–nitrate process	873	10	33.88 ± 0.51	66.12 ± 0.99
			973	15	32.95 ± 0.49	67.05 ± 1.00
			973	365	32.19 ± 0.48	67.81 ± 1.02
			973	870	33.92 ± 0.51	66.07 ± 0.99
			1073	10	33.45 ± 0.50	66.55 ± 0.10

Noteworthy, regardless of the chosen synthetic method, Cs_2O–Al_2O_3 ceramic samples containing 20 or 33 mol % cesium oxide prepared at lower temperatures have the tailored amounts of Cs_2O (to the error bar of the method).

CONCLUSIONS

Conditions have been considered to manufacture Cs_2O–Al_2O_3 ceramic samples containing 20 and 33 mol % cesium oxide by ceramic technique and by glycine–nitrate combustion process with various isothermal exposure parameters. The heat treatment of the batch at 773 K is insufficient, and in addition to an X-ray amorphous phase, diffraction peaks characteristic of unreached precursors appear on the X-ray diffraction patterns. Batch calcination at 1373 K leads to the complete vaporization of cesium from the sample. The phase composition, elemental composition as analyzed by X-ray fluorescence spectroscopy, and surface morphology of the prepared samples show that ceramic technique and glycine–nitrate combustion process are advised for preparing Cs_2O–Al_2O_3 samples. The optimal parameters for the heat treatment of the batch to prepare Cs_2O–Al_2O_3 samples are a temperature of 973 K and calcination time of 365 h when standard solid-phase technology is used and 870 h for the glycine–nitrate combustion process.

ACKNOWLEDGMENTS

The authors express their gratitude to the staff of the resource centers "X-ray Diffraction Methods of Investigation", "Interdisciplinary Resource Centre for Nanotechnology", "Innovative Technologies of Composite Nanomaterials", and "Geomodel" of the science park of St. Petersburg State University.

FUNDING

This work was supported by Ministry of Education and Science of the Russian Federation (project No. 075-15-2021-1383).

CONFLICT OF INTEREST

The authors declare that they have no conflicts of interest to disclose here.

REFERENCES

1. R. Prins, J. Catal. **392**, 336 (2020). https://doi.org/10.1016/j.jcat.2020.10.010
2. G. Busca, Prog. Mater. Sci. **104**, 215 (2019). https://doi.org/10.1016/j.pmatsci.2019.04.003
3. C. Meephoka, C. Chaisuk, P. Samparnpiboon, and P. Praserthdam, Catal. Commun. **9**, 546 (2008). https://doi.org/10.3390/cryst11060690
4. P. S. Shreyas, B. P. Mahesh, S. Rajanna, and N. Rajesh, Mat. Tood. Proc. **45**, 429 (2021). https://doi.org/10.1016/j.matpr.2020.12.1012
5. L. I. Podzorova, A. A. Ilyicheva, O. I. Penkova, O. S. Antonova, A. S. Baikin, and A. A. Konovalov, Inorg. Mater. **55**, 671 (2019). https://doi.org/10.1134/S0020168519060128
6. W. Chaitree, S. Jiemsirilers, O. Mekasuwandumrong, et al., Catal. Today **164**, 302 (2011). https://doi.org/10.1016/j.cattod.2010.11.004
7. S. V. Tsybulya and G. N. Kryukova, Phys. Rev. B **77**, 024112 (2008). https://doi.org/10.1103/PhysRevB.77.024112
8. G. Paglia, C. E. Buckley, A. L. Rohl, et al., Phys. Rev. B **68**, 144110 (2003). https://doi.org/10.1103/PhysRevB.68.144110
9. M. Rudolph, M. Motylenko, and D. Rafaja, IUCrJ **6**, 116 (2019). https://doi.org/10.1107/S2052252518015786
10. B. Marí, K. C. Singh, M. Moya, et al., Opt. Quant. Electron. **47**, 1569 (2015). https://doi.org/10.1007/s11082-014-9997-9
11. M. N. Saeed Adel, Q. A. Al-Gunaid Murad, N. K. Subramani, et al., Pol.-Plast. Tech. Eng. **57**, 1188 (2018). https://doi.org/10.1080/03602559.2017.1373402
12. P. F. McMillan, A. Grzechnik, and H. Chotalla, J. Non-Cryst. Solids **226**, 239 (1998). https://doi.org/10.1016/S0022-3093(98)00416-5
13. K. Fukumi, S. Sakka, and T. Kokubo, J. Non-Cryst. Solids **93**, 190 (1987). https://doi.org/10.1016/S0022-3093(87)80038-8
14. N. Macleod, J. M. Keel, and R. M. Lambert, Catal. Lett. **86**, 51 (2003). https://doi.org/10.1023/A:1022602807322
15. A. A. Ansari, M. A. M. Khan, M. N. Khan, and S. A. Alrokayan, J. Semicond. **32**, 1 (2011). https://doi.org/10.1088/1674-4926/32/4/043001
16. C. Guéneau and J. L. Fleche, CALPHAD: Comput. Coupling Phase Diagrams Thermochem. **49**, 67 (2015). https://doi.org/10.1016/j.calphad.2015.02.002
17. V. L. Stolyarova, V. A. Vorozhtcov, S. I. Lopatin, et al., Rapid Commun. Mass Spectrom. **35**, e8829 (2021). https://doi.org/10.1002/rcm.9079
18. V. L. Stolyarova, V. A. Vorozhtcov, S. I. Lopatin, et al., Rapid Commun. Mass Spectrom. **35**, e9097 (2021). https://doi.org/10.1002/rcm.9097
19. O. S. Kaimieva, I. E. Sabirova, E. S. Buyanova, and S. A. Petrova, Russ. J. Inorg. Chem. **67**, 1211 (2022). https://doi.org/10.1134/S0036023622090054
20. A. E. Medveeva, E. V. Makhonina, L. S. Pechen, et al., Russ. J. Inorg. Chem. **67**, 952 (2022). https://doi.org/10.1134/S0036023622070154
21. E. V. Babaev, Russ. J. Gen. Chem. **80**, 2590 (2010). https://doi.org/10.1134/S1070363210120261

22. M. J. O'Donnell, C. Zhou, and W. L. Scott, J. Am. Chem. Soc. **118**, 6070 (1996). https://doi.org/10.1021/ja9601245

23. T. L. Simonenko, N. P. Simonenko, E. P. Simonenko, et al., Russ. J. Inorg. Chem. **67**, 1495 (2022). https://doi.org/10.1134/S0036023622600939

24. O. B. Tomilin, E. E. Muryumin, M. V. Fadin, et al., Russ. J. Inorg. Chem. **67**, 431 (2022). https://doi.org/10.1134/S0036023622040192

25. J. Wang, H. Zhao, and Y. Wen, Electrochim. Acta **113**, 679 (2013). https://doi.org/10.1016/j.electacta.2013.09.086

26. V. D. Zhuravlev, V. G. Vasil'ev, E. V. Vladimirova, et al., Glass Phys. Chem. **36**, 506 (2010). https://doi.org/10.1134/S1087659610040164

27. F. Cardarelli, *Materials Handbook* (Springer-Verlag, London, 2008).

28. R.-S. Zhou and R. Snyder, Acta Crystallogr., Sect. B: Struct. Sci. **47**, 617 (1991). https://doi.org/10.1107/S0108768191002719

29. G. Langlet, C. R. Acad. Sci. **259**, 3769 (1964).

Translated by O. Fedorova